Journal of Zhejiang University-SCIENCE B (Biomedicine & Biotechnology)
ISSN 1673-1581 (Print); ISSN 1862-1783 (Online)
www.jzus.zju.edu.cn; www.springerlink.com
E-mail: jzus@zju.edu.cn

Assessment of cortical bone microdamage following insertion of microimplants using optical coherence tomography: a preliminary study*

Hemanth Tumkur LAKSHMIKANTHA[§1], Naresh Kumar RAVICHANDRAN[§2], Mansik JEON[†‡2], Jeehyun KIM[2], Hyo-sang PARK[†‡1]

[1]*Department of Orthodontics, School of Dentistry, Kyungpook National University, Daegu 41940, Korea*

[2]*School of Electronics Engineering, College of IT Engineering, Kyungpook National University, Daegu 41566, Korea*

[†]E-mail: msjeon@knu.ac.kr; parkhs@knu.ac.kr

Received Dec. 13, 2017; Revision accepted Feb. 5, 2018; Crosschecked Oct. 10, 2018

Abstract: Objectives: The study was done to evaluate the efficacy of optical coherence tomography (OCT), to detect and analyze the microdamage occurring around the microimplant immediately following its placement, and to compare the findings with micro-computed tomography (μCT) images of the samples to validate the result of the present study. Methods: Microimplants were inserted into bovine bone samples. Images of the samples were obtained using OCT and μCT. Visual comparisons of the images were made to evaluate whether anatomical details and microdamage induced by microimplant insertion were accurately revealed by OCT. Results: The surface of the cortical bone with its anatomical variations is visualized on the OCT images. Microdamage occurring on the surface of the cortical bone around the microimplant can be appreciated in OCT images. The resulting OCT images were compared with the μCT images. A high correlation regarding the visualization of individual microcracks was observed. The depth penetration of OCT is limited when compared to μCT. Conclusions: OCT in the present study was able to generate high-resolution images of the microdamage occurring around the microimplant. Image quality at the surface of the cortical bone is above par when compared with μCT imaging, because of the inherent high contrast and high-resolution quality of OCT systems. Improvements in the imaging depth and development of intraoral sensors are vital for developing a real-time imaging system and integrating the system into orthodontic practice.

Key words: Optical coherence tomography; Microimplant; Cortical bone; Micro-computed tomography
https://doi.org/10.1631/jzus.B1700612 **CLC number:** R783

1 Introduction

Anchorage control is an imperative factor in the success of orthodontic treatment (Park et al., 2006). In recent times, microimplants have gained immense popularity and have developed into a reliable source of absolute osseous anchorage. Primary stability is one of the most important factors to be considered for the success of microimplants and can be measured by evaluating its insertion torque, removal torque, and pull-out strength (Wilmes et al., 2006). Bone quality, the design and size of the microimplants, and the

‡ Corresponding authors
§ The two authors contributed equally to this work
* Project supported by the BK21 Plus Project Funded by the Ministry of Education, Korea (No. 21A20131600011) and the Industrial Infrastructure Program of Laser Industry Support Funded by the Ministry of Trade, Industry & Energy, Korea (No. N0000598)
ORCID: Hemanth Tumkur LAKSHMIKANTHA, https://orcid.org/0000-0002-9634-9420; Naresh Kumar RAVICHANDRAN, https://orcid.org/0000-0002-3712-5304; Mansik JEON, https://orcid.org/0000-0002-0630-9039; Hyo-sang PARK, https://orcid.org/0000-0003-0227-4112

preparation of the implantation site all have great impact on the primary stability of the microimplants. Initially, the stability of the microimplants depends solely on the mechanical interlocking of the threads of the implants with the surrounding bone (Melsen and Costa, 2000). This interlocking mechanism, however, causes extensive damage to surrounding bone and presents in the form of diffuse damage and distinct linear microcracks on the bone around the microimplants (Lee and Baek, 2010; Shank et al., 2012). A high amount of microdamage can lead to a reduction of bone-implant contact after remodeling and this may lead to dislodgement of microimplants (Lee and Baek, 2010). It is imperative to decrease the formation of these microcracks in order to improve the primary stability of microimplants. Past studies on the issue of microcracks are based on clinical observations backed by micro-computed tomography (μCT), histomorphometric analysis (Wawrzinek et al., 2008), and finite element analysis (FEA) studies (Motoyoshi et al., 2009). The main drawback of the studies is that they were invasive on the bone or were biomechanical analysis models simulating the stress patterns on the bone. Therefore, we chose to utilize a non-invasive and non-destructive imaging system with high resolution and high contrast, such as the optical coherence system, to visualize and analyze the microcrack formation on the bone around the microimplants.

Optical coherence tomography (OCT) is an imaging system which provides volumetric and cross-sectional images to disclose the internal structure of biological tissues non-invasively and non-destructively (Bakhsh et al., 2013). OCT is based on the more than 100-year-old principle of Michelson interferometry. The technique was first introduced by Fercher et al. (1988) and Huang et al. (1991), for investigation of the human eye. Application of OCT as a non-invasive imaging tool has been used in ophthalmology (Carrasco-Zevallos et al., 2016; Zhang et al., 2016; Shirazi et al., 2017), agronomy (Ravichandran et al., 2016a, 2016b; Wijesinghe et al., 2017), entomology (Choi et al., 2017; Ravichandran et al., 2017), and industrial inspection (Shirazi et al., 2016) and has been studied for more than two decades. In the field of orthodontics, it has proven to be of value for visualization of changes in the enamel surface after routine orthodontic de-bonding and various demineralization procedures (Koprowski et al., 2014; Pithon et al., 2015; Wijesinghe et al., 2016; Seeliger et al., 2017). The ability of the system to provide a 3-dimensional (3D) image and also 2-dimensional (2D) images with high sub-micron resolution is of note. The possibility of real-time imaging makes it an exciting new system in the field of orthodontic research.

As far as we know, no previous studies have utilized OCT to assess the microdamage associated with placement of orthodontic microimplants. This preliminary study is the first of its kind to evaluate the occurrences and prevalence of microdamage around the microimplant immediately after its placement onto the cortical bone. Thus, the aim of the study was to: (1) to present OCT images showing the microdamage occurrences around the microimplant, and (2) to compare OCT images with μCT images, in order to evaluate the efficacy of OCT for examining cortical bone microdamage.

2 Materials and methods

2.1 Experimental setup

Fresh bovine rib segments were harvested and were cut into workable smaller pieces to serve as placement sites of microimplants. The periosteum was removed and the segments were stored in saline until use. A previous study has shown that 2 mm of cortical bone is necessary for placement of microimplants (Fernandes et al., 2015). Bovine ribs present with the same architectural pattern as that of the human mandibular bone (Bredbenner and Haug, 2000). They have shown that the bovine rib is similar to the human mandible, with a clear definition of cortical and cancellous bone and can be used as a material of choice in studies focusing on maxillofacial implantation. A total of 20 conical-shaped titanium self-drilling microimplants of the AbsoAnchor System (Dentos, Daegu, Korea) with identical design were selected for this study. Each of the microimplants was 9 mm in length and had a diameter of 1.5 mm. The self-drilling microimplants were inserted at an angle of 90° and 45° onto the bone segments using the tools provided by the company, as shown in Fig. 1. The microimplants were inserted by a trained operator. A battery-operated hand-piece for implant insertion was not used, so as to replicate the stresses exerted on the bone surface by operator insertion of the microimplant. During the

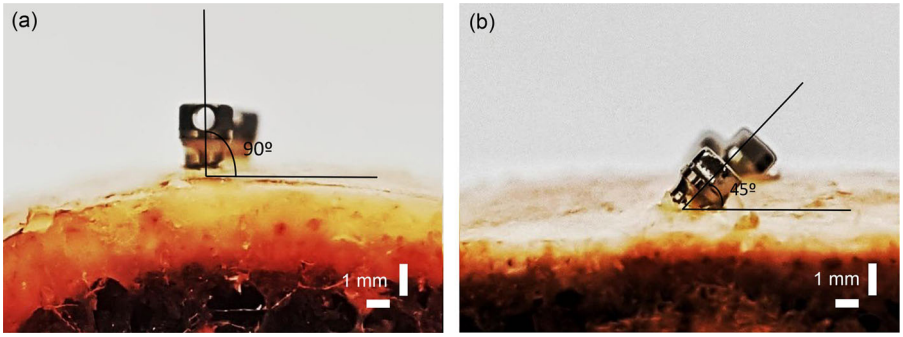

Fig. 1 Representative images of microimplant insertion onto the cortical bone surface
Microimplant was inserted at an angle of 90° (a) and 45° (b) to the cortical bone surface

microimplant mounting process, we used an angle measurer as a guide during placement of microimplant onto the bone surface. Furthermore, we measured the post-insertion torque of all our microimplants and found it to be within the acceptable range of insertion torque (7–10 N·cm) for bovine bone with a thickness of 2 mm. Hence, we can deduce that no additional stresses were incorporated during microimplant placement.

Following microimplant insertion, the bone segment along with the microimplant was mounted on an acrylic segment to stabilize it from untoward movement during scanning.

2.2 Optical coherence tomography

2.2.1 OCT specification

In this study, a commercial spectral OCT system (OCS1310V1; Thorlabs, Newton, NJ, USA) producing cross-sectional (2D) and volumetric (3D) optical imaging (Fig. 2) was used. It is connected to a preconfigured personal computer and the images are obtained with a scanner probe. The commercial system had a center wavelength of 1300 nm with a spectral bandwidth of >97 nm, and the axial resolution of the system can be attained at <16 μm and a transverse resolution of 25 μm. The scan range used for this experiment for every 2D image was 4 mm. The 3D volumetric image acquisition was 4 mm×4 mm. The OCT system produces 3D images by combining several 2D scans of the area of interest, allowing analysis of the surface structure of the sample and in-depth analysis of the scanned structures. OCT images were taken to evaluate the cortical bone structure before and after insertion of microimplant (2D and 3D).

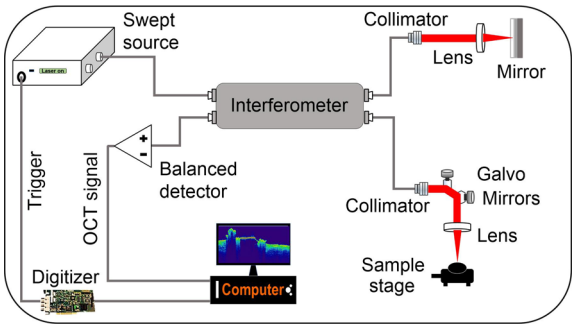

Fig. 2 SS-OCT system schematic diagram
Schematic representation of the 1300 nm swept-source optical coherence tomography (SS-OCT) system used for the experiment

2.2.2 A-scan analysis algorithm

After completion of the initial scanning process, the images were processed by volume rendering software and a 3D model of the sample was obtained. The scan range was 4 mm×4 mm with an obtained depth information of 2 mm. To analyze the OCT images, a MATLAB program (MATLAB 2014a, the MathWorks, Natick, MA, USA) was developed and adopted for OCT image intensity analysis (A-scan analysis). A median filter of 2×2 was applied to the selected OCT image to reduce the noise within the image. The algorithm programmed into the MATLAB software sequentially analyzed the 2D OCT images, and plotted intensity peaks. The procured intensity profiles are normalized and plotted for clarity. Intensity analysis is done for OCT images in the horizontal and vertical directions of the image. Based on the final plot provided by the A-scan, we can correlate the intensity variations to the various structures seen on the images, thereby enabling us to analyze the cracks, bone debris, implant surface, and other structural properties of the samples.

2.3 Micro-computed tomography imaging

The 3D microstructure of the bone sample was assessed by μCT (Skyscan 1076, Skyscan, Kontich, Belgium) using a 15-μm low-contrast resolution, which was powered by a sealed X-ray source of 20–100 kV with a spot size of less than 5 mm (4 W). The camera pixel size of μCT was 12.25 μm and source voltage was 100 kV. Exposure was for 680 ms and the rotation step was 0.600°. The scanning motion was step and shoot. The single scan duration was 24.26 min and radiation safety was less than 1 μSv/h at any point on the instrument surface during the scan. Total size of the scanning volume was 17 mm (length) per single scan length. Image processing was performed using volume rendering software on a personal computer. The acquired images were visually aligned with the OCT images to obtain a qualitative comparison.

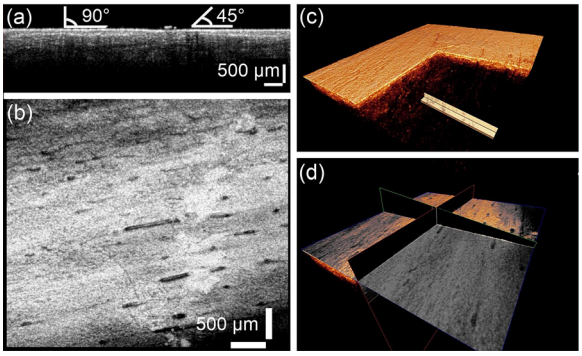

Fig. 3 2D and 3D images of the control area imaged using SS-OCT system

(a) 2D OCT image of the bone sample, with the arbitrary location of implant placement. (b) En face image obtained at 100 μm from the bone surface. (c) 3D OCT image of the control surface, which was an orthogonally sectioned view of internal structural variations. (d) 3D image along with orthogonal section planes with en face. Angulations of 90° and 45°, shown in (a), give a representative arbitrary placement of microimplants

3 Results

3.1 Imaging of the bone specimens using OCT

For the evaluation of the samples, the OCT images were obtained before microimplant insertion and after placement of the implant on the surface of the prepared bone sample. Images were obtained in both 2D (longitudinal section) and 3D imaging modes. To maintain uniformity in the scanning procedure, all the samples were scanned covering an area of 4 mm×4 mm, with the implant in the center of the image. Volume rendering software is used to create an en face image and for further structural analysis. Fig. 3 shows the representative images of the control area in the cortical bone, before the insertion of the microimplants. The 2D, en face, 3D, and 3D image with orthogonal section plane of a representative cortical bone sample are shown in Figs. 3a–3d. At the initial evaluation of the cortical bone surface structure, examination by OCT before insertion of the microimplant showed the typical anatomy of the bone surface. Most of the images showed only the cortical bone in the 2D and 3D models (Fig. 3). Imperfections on the surface of the bone are clearly visible and this can serve as a control while evaluating microcracks.

Fig. 4 shows the representative OCT images of the microimplant implant inserted at an angle of 45° onto the cortical bone surface. Fig. 4a is a representative photograph of the implant mounted on the bovine bone at an angle of 45°. Fig. 4b is the 3D rendered volumetric image obtained to visualize and analyze the occurrence of microcracks around the microimplant at different depths. Figs. 4c and 4d show the cross-section 2D images and the microcrack is observed as it progresses through a single plane. Figs. 4e and 4f are en face images extracted from the 3D volume at 100 and 50 μm depth, respectively. The microcracks presenting parallel to the cortical bone surface can be observed in these images. The areas in light blue represent an intensity drop in the OCT image and at a higher intensity, the color map changes to yellow and subsequently to red. These indicate the visualized structural changes in images. As the implant is a titanium alloy, it has high reflectivity. Because of the high reflectivity of the microimplant, the OCT system cannot provide adequate penetrated depth information in relation to the microimplants. Thus, the implant is shown as to be of a dark blue hue. Following oblique insertion of the microimplant, the area on the surface of the cortical bone, corresponding to the area distal to the implant, cannot be adequately visualized, as the laser source used in OCT to scan cannot penetrate through the microimplants, and thus is being portrayed to be of a dark blue hue.

Fig. 5 illustrates the scanned swept-source optical coherence tomography (SS-OCT) images of a microimplant inserted at an angle of 90° on the cortical

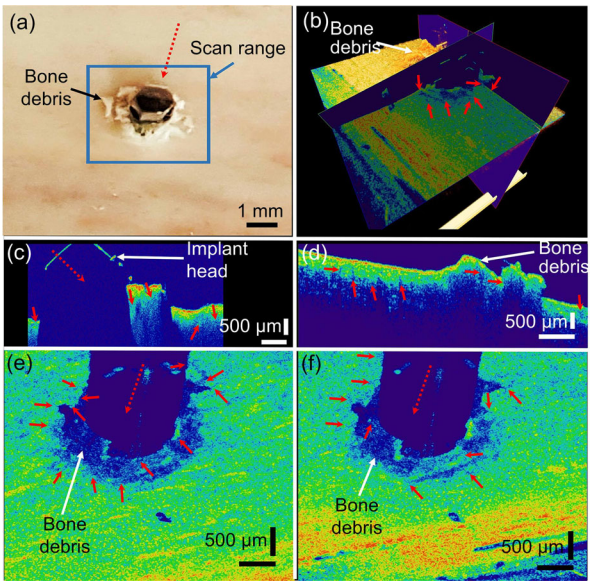

Fig. 4 Representative 2D and 3D SS-OCT images of an implant inserted at 45° to the cortical bone surface
(a) An added representative camera photograph of the implant mounted in a bone. (b) A 3D image with sectional planes in all three directions. (c, d) 2D OCT images show the cross-section of the sample along with the orthodontic implant. (e, f) En face images at 100 and 50 μm depth, respectively. Red arrows shown in the images indicate the location of microcracks around the microimplant. The red dotted arrows indicate the direction of implant insertion on to the bone

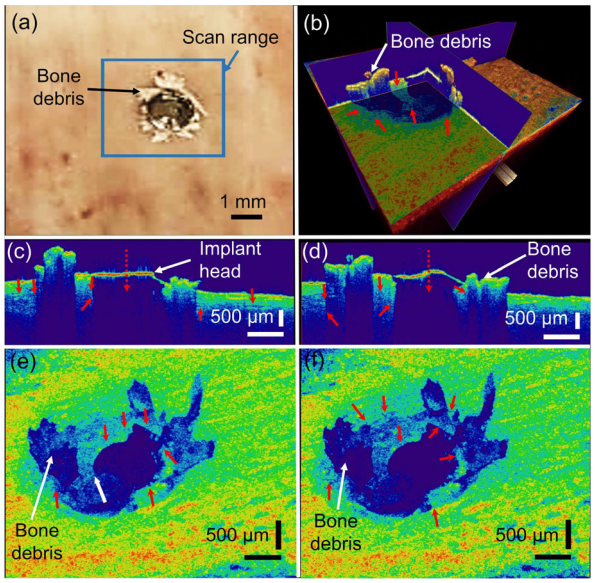

Fig. 5 Representative 2D and 3D SS-OCT images of an implant inserted at 90° to the cortical bone surface
(a) An added representative camera photograph of the implant mounted in a bone. (b) A 3D image with sectional planes in all three directions. (c, d) 2D OCT images show the cross-section of the sample along with the orthodontic microimplant. (e, f) En face images at 50 and 100 μm depth, respectively. Red arrows shown in the images indicate the location of microcracks around the microimplant. The red dotted arrows indicate the direction of implant insertion onto the bone

bone surface. Fig. 5a shows the photograph of the implant mounted at 90° to the sample surface. Likewise, Fig. 5b is a 3D volumetric OCT image with sectional planes in all directions, followed by Figs. 5c and 5d, which are 2D cross-sectional OCT images. Figs. 5e and 5f are the en face images extracted from the volumetric image at a depth of 50 and 100 μm respectively. All the solid red arrows in the images Figs. 5b–5f are used to present the location of the substantial microcracks.

Figs. 4 and 5 represent the cortical bone structure after insertion of the microimplant. The area of microdamage occurring to the bone, caused by microimplant insertion, is distinctly visible on the OCT images. In the OCT image presentation, microdamage to the bone is seen as areas of different intensities and elevations on different planes as compared to the surrounding normal bone surface. These affected areas are seen around the implant surface and propagate to a depth of up to 1 mm as shown in Figs. 4b, 4e, 4f, 5b, 5e, and 5f. The presence of microcracks, occurring as a severe form of microdamage, is evident on the scanned images as represented in Figs. 4 and 5. Numerous microcracks emanating around the implant are seen on the images. In the 2D images, visualization of the number of microcracks propagated up to a distance of up to 1 mm from the implant is seen in Figs. 4e, 4f, 5e, and 5f. In the 3D images, presentation of the microcracks around the insertion zone of the microimplants on the surface of the cortical bone is seen in Figs. 4b, 4e, 4f, 5b, 5e, and 5f.

In Fig. 6, the en face images used for A-scan analysis were taken at a depth of 83 μm from the bone surface. As A-scan plots are intensity-dependent plots, and the microcracks are a discontinuity in the bone structures, they will be seen as a sudden drop in intensities in the A-scan plot. It is seen from the A-scan plots that the microcracks (sudden intensity drops) around the 45° angulated microimplants are higher in number than those around the 90° angulated microimplants.

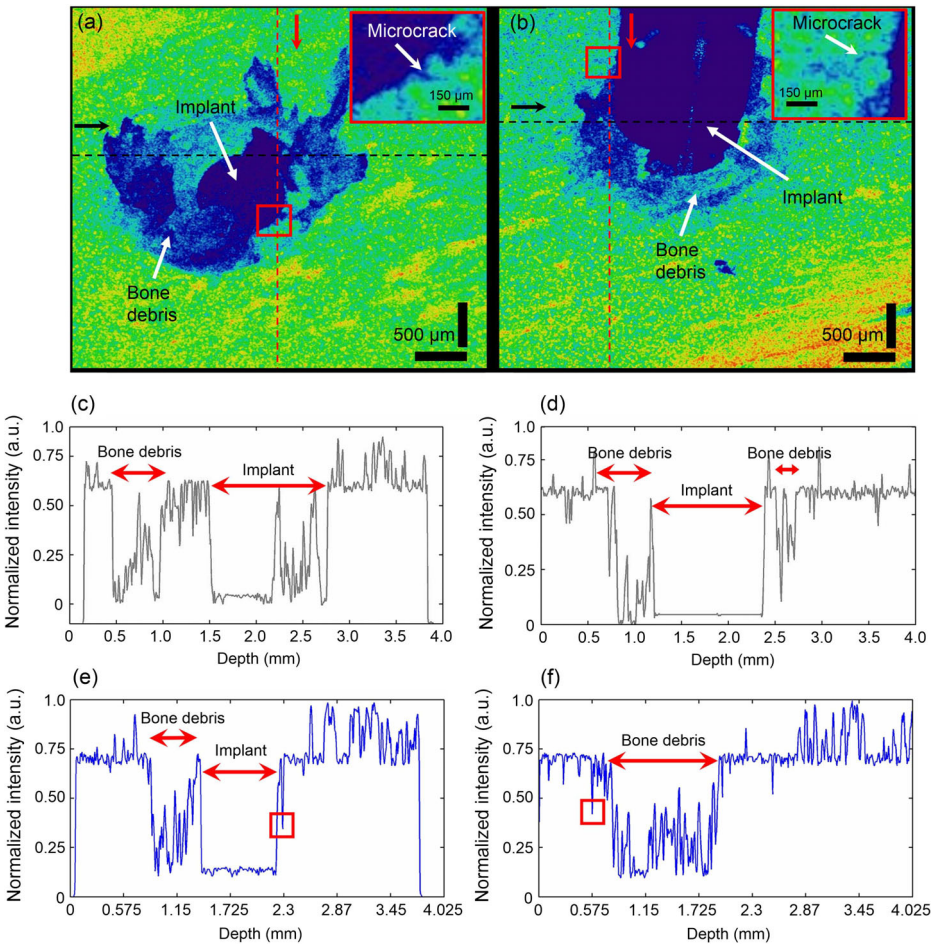

Fig. 6 A-scan plot analysis and microcrack and microdamage identifications for en face OCT images of 90° and 45° angulated insertions of microimplants on the cortical bone surface

(a) and (b) are the en face OCT images of the 45° and 90° angulated microimplant OCT images, respectively. (c) and (d) are the horizontal A-scan plots obtained from (a) and (b), respectively. Similarly, (e) and (f) are the vertical A-scan plots obtained from (a) and (b), respectively. Their corresponding crack is identified in their A-scan plots. The direction of obtained A-scan is represented by black and red arrows in the en face images. Also, the precise location at which the A-scan in the OCT images was obtained is represented with black and red dotted lines for their respective horizontal and vertical directions, respectively. A clear representative crack in the en face images of 45° and 90° angulated microimplant OCT images is shown as red box. The inset images at the top right region in (a) and (b) are the magnified areas, which are represented by a red box region in their respective en face images. Clear and distinct microcracks around the bone-implant interface are represented in the inset indicated by a white arrow. In the A-scan plots (e, f), the red box regions correspond to the indicated microcracks in the respective inset images

3.2 μCT representation of the bone specimens

Fig. 7 is the μCT image of the cortical bone structure after insertion of the microimplant. Figs. 7a, 7c, and 7e are 3D, 2D, and en face images of the microimplant inserted at an angle of 45° on the cortical bone surface, respectively and Figs. 7b, 7d, and 7f are 3D, 2D, and en face images of the microimplant inserted at an angle of 90°, respectively. Microimplant and the surrounding bone architectures could be effectively visualized in 3D reconstruction and en face images with the use of μCT. In the cross-sectional view, the sense cortical bone and trabecular bone patterns can be appreciated owing to the excellent depth penetration and good resolution of μCT. The bone surrounding the microimplant and the clear discontinuities in the cortical bone structure can be well appreciated emanating around the entire length of the microimplant owing to the high opacity of microimplants on the images. Such details are not

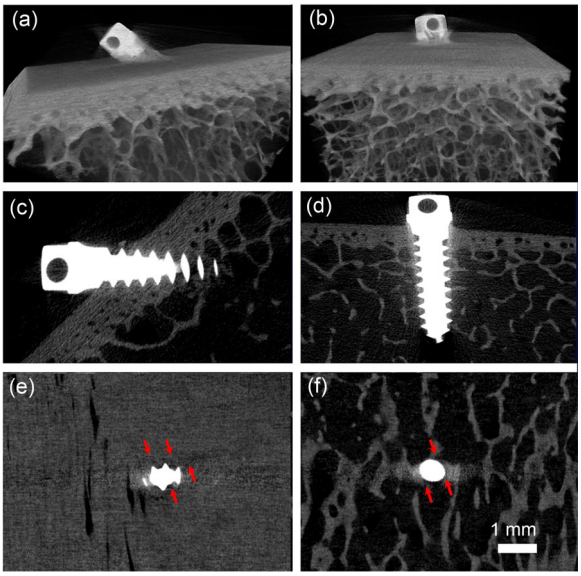

Fig. 7 Representative 2D and 3D μCT images of a microimplant inserted to the cortical bone surface at 45° (a, c, e) and 90° (b, d, f) angulations
(a, b) 3D images showing cortical and trabecular bone. (c, d) 2D μCT images showing the cross-section of the sample along with the microimplant. (e, f) En face images at 100 μm depth. Red arrows indicate the location of microcracks around the microimplant

visible on the OCT images because of its poor penetration through the tissues. In addition to the microcracks, visualization of the micro-elevations and the accumulation of bone debris can be well observed on the μCT images.

3.3 Comparison between OCT and μCT

Fig. 8 represents the images for the two imaging modalities. Figs. 8a and 8c show 2D and en face images of the sample imaged with OCT, respectively and Figs. 8b and 8d show 2D and en face images of the sample imaged with μCT, respectively. In our study we found that, whilst the μCT system is adequate to image deeper lying structures, the OCT system offers more contrast and therefore more image detail of hard tissue at comparable nominal resolutions. As the arrows indicate, a clear discontinuity is seen in the cortical bone surface around the microimplant, representing a microcrack. Numerous microcracks are seen emanating around the microimplant when imaged in both modalities. In Figs. 8e and 8f, accumulation of bone debris (1) and micro-elevations (2) of the cortical bone surface due to implant placement can be appreciated.

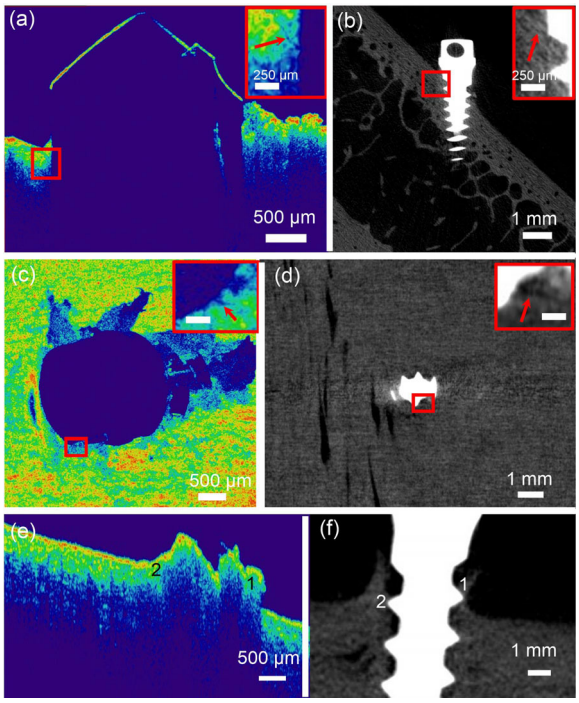

Fig. 8 Comparisons of images obtained from OCT and μCT
2D (a) and en face (c) images of the bone sample scanned with OCT. 2D (b) and en face (d) images of the bone sample scanned with μCT. Presentation of bone debris (1) and micro-elevations (2) seen around the microimplant on the OCT (e) and μCT (f) images. Red arrows indicate the occurrences of microcracks around the microimplant. Inset images are magnified areas representative of red box regions in (a–d)

4 Discussion

The purpose of this qualitative study was to demonstrate the use of OCT for characterization of cortical bone surface microcrack presentation following placement of an orthodontic microimplant and then compare the resultant images with μCT.

The findings from the study indicate that OCT can be used as a non-invasive method for imaging the microdamage occurring around the microimplant following immediate placement.

At the initial evaluation of the cortical bone surface structure, OCT before insertion of the microimplant showed the typical anatomy of the bone surface. Most of the images showed only the cortical bone in the 2D and 3D models (Fig. 3). Imperfections on the surface of the bone are clearly visible and this

can serve as a control while evaluating microcracks. Depth penetration of OCT is insufficient in relation to bony tissues. With the use of OCT, in our study, we obtained a depth penetration of up to 250 μm. Based on previous FEA studies, we can derive a conclusion that stress accumulation during immediate placement of the microimplant is at a maximum at the surface of the cortical bone. With this in mind, even though the penetration of the OCT system is not sufficient to image the microimplant in its entirety, it provides excellent images of high resolution of the surface of the cortical bone.

Primary stability of the microimplants depends on a number of factors. Quality of the bone is an important factor determining the primary stability. Microimplants placed in the mandible have higher failure rates owing to the increased density of the cortical bone as compared to in the maxilla. Other factors like insertion torque and microimplant design also play an important role in primary stability. Insertion of the microimplant into the bone surface leads to occurrence of microdamage on the bone. These areas of microdamage can have a marked effect on the primary and secondary stability of the microimplant. Use of a microimplant on a dense cortical bone, or insertion with a high torque and incorrect angulations may lead to formations of large microcracks. These microcracks act as areas of demineralization or voids and hamper the primary stability of the microimplant. Furthermore, as the bone around the microimplant heals, these areas represent bone of much lesser density than the surrounding bone and can affect the areas of stress patterns occurring around the microimplant, leading to loosening of the microimplant, especially when axial or torsional forces are applied.

The area of microdamage occurring to the bone caused by mini-screw implant insertion is distinctly visible on the OCT images. In the OCT image, microdamage to the bone is seen as areas of different intensity and elevations on different planes as compared to the surrounding normal bone surface. These affected areas are seen around the implant surface and propagate to an area of up to 1 mm as shown in Figs. 4b, 4e, 4f, 5b, 5e, and 5f. Areas of bone-damage can develop into areas of demineralization and represent an area of weaker and more damaged bone than the surrounding bone structure and can impact the primary stability of the microimplants (Yadav et al., 2012). The area of diffuse microdamage on the bone is more severe when the implant is inserted at an angle of 45° than when inserted at an angle of 90° since with oblique insertion of microimplants there is an increase in contact area between the screw and the cortical bone (Woodall et al., 2011). OCT presents a unique advantage for visualization and analysis of the presented microdamage of the bone structure. Since the images generated can be modeled into a 3D model, visualization of the diffuse microdamage can be presented in all three plans and can be analyzed in its entirety quantitatively.

Fig. 6 represents an A-scan analysis of the OCT images. An A-scan analysis was performed, using MATLAB coding, to confirm and evaluate the presence of microcracks around the bone-implant interface. The sudden drop in the intensity corresponds to the discontinuity in the bone structure around the implant, validating the visualization of microcracks present in the 3D model. This feature of OCT sets it apart from other commonly used imaging modalities, as quantitative analysis pertaining to the nature of the microcrack can be obtained. It was beyond the scope of the present study to quantitatively evaluate the microcracks. Further volumetric studies need to be done to analyze the microcracks in their entirety.

μCT, of late, is considered the gold standard for assessing bone morphology and microstructures (Hsu et al., 2014). Dental CT has been used widely in clinical practice and for research purposes. The main advantages it possesses are that it is inexpensive when compared to μCT and that it involves low radiation doses. However, it is dependent on scanning position and the image quality can be affected (Katsumata et al., 2007; Nackaerts et al., 2011). On the other hand, image quality associated with μCT is of a high resolution and in excellent detail. However, the radiation exposure associated with μCT is very high. The ionizing effects of the radiation can have an effect on samples. Secondly, the μCT imaging technique relies on contrast, brightness, and signal to noise ration. These parameters are sensitive and can lead to alterations in the image quality. Some imaging artifacts are peculiar to CT, such as ring artifacts and beam hardening, and can affect the overall quality of the image. As in our study, the image quality of OCT was on a par with that of μCT. Depth penetration of μCT

through the tissues was far superior to OCT. Images produced by both imaging modalities can be constructed into a 3D model and can be analyzed as such. Park et al. (2017) compared the diagnostic accuracies of OCT, μCT, and histology in periodontal disease. In their study, the researchers compared the OCT images obtained from periodontal disease and compared them to μCT images and histological sections. The study suggested that when compared with OCT, μCT presents images with less visual acuity. Moreover, μCT involves a high radiation dosage compared to the non-invasive, nondestructive imaging modality of OCT.

4.1 Comparisons of OCT and μCT images to visualize bone microdamage

As seen in Fig. 8, the image quality obtained by OCT is on a par with that of μCT. In 2D and en face scans, presentation of microdamage to the cortical bone is clearly evident in both modalities. Microcracks are seen as distinct discontinuities in the opaque intensity of the cortical bone around the microimplant. The high contrast of the microimplant might hinder the identification of microcracks, whereas in OCT images, because of the dark hue of the microimplant, it is easier to identify microcracks on the cortical bone surface. Areas of micro-elevation of the cortical bone can be well appreciated especially in the angulated placement of the microimplant. This phenomenon is better seen in OCT images as the resolution of the images is higher, especially at the surface of the cortical bone. Presentation of microdamage closer to the surface of the cortical bone is better represented in the OCT images because of higher resolution and better contrast of the system. Presence of bone debris around the microimplant is well appreciated in both imaging modalities. At surface-near positions of OCT images, the structure of cortical bone seems to show slightly higher contrast than seen in μCT. Finally, processes of bone mineralization and demineralization over extended periods of time can be observed without ionizing radiation.

Higher axial resolution of up to 1–2 μm with 800 nm center wavelength OCT systems, given with appropriate bandwidth of the source, will enable visualization of the cracks in higher resolution in real time, in vivo, and without the harmful radiation exposure of μCT systems. Recent developments in OCT systems mean that there is a reduced sample arm size and an overall reduction in system size that can be effectively integrated into orthodontics. Future system developments should be aimed at modifying the system to aid in day-to-day orthodontic practice.

Various methods of imaging have been used previously to assess microdamage on the cortical bone surface. Some of the commonly used modalities are dental radiography, fluorescence imaging (Yadav et al., 2012), and histological studies (Nguyen et al., 2017). In studying microdamage, we need to bear in mind that the microcracks present in the cortical bone are a 3D entity and need to be studied as such. Histological sections provide quality images but are destructive to the tissues and the analysis is restricted to a single plane since the sections of tissues can only be performed in one plane. However, with the use of OCT, a 3D image of the desired area can be obtained without any damage to the tissues and can be analyzed as such.

4.2 Limitations

As with other imaging modalities, OCT systems do present certain limitations. Due to its use of light waves, the penetration depth of the system is below par when compared to other imaging modalities, but the superior image resolution and contrast make it invaluable during imaging of surface structures of tissues. One of the future directions of OCT system development is towards improvement of depth penetration of the system. Patient cooperation becomes an important factor during use of OCT in in vivo studies. Any movement of the subject can diminish the quality of the image. With newer machines, acquisition time is shorter, which may result in fewer motion-related artifacts. Also, a case of usability of currently available OCT systems for an orthodontic microimplant treatment procedure could be achieved by surgically making an incision in the soft tissues. This will make it possible to use OCT for directly scanning on to the bone surface.

5 Conclusions

OCT represents an interesting alternate to μCT and other non-invasive imaging modalities used in

detection of microdamage on the cortical bone following immediate placement of a microimplant. OCT can achieve the best resolution of all known non-invasive imaging methods and is non-destructive to tissues being studied, capable of producing images that can be processed and studied as a 3D model. Furthermore, with technical advancement, real-time imaging of the bone surface can be achieved, especially since no harm is done to the patient due to OCT's non-invasive and non-radiative qualities. Further studies need to be made using the full spectrum of options available with OCT imaging.

Contributors

The experimental idea was proposed by Hyo-sang PARK. Sample preparation, experiments, and data analysis were carried out by Hemanth Tumkur LAKSHMIKANTHA and Naresh Kumar RAVICHANDRAN. Results and their confirmation were given by Hyo-sang PARK, Mansik JEON, and Jeehyun KIM. All authors had equal contribution for manuscript preparation.

Compliance with ethics guidelines

Hemanth Tumkur LAKSHMIKANTHA, Naresh Kumar RAVICHANDRAN, Mansik JEON, Jeehyun KIM, and Hyo-sang PARK declare that they have no conflict of interest.

This article does not contain any studies with human or animal subjects performed by any of the authors.

References

Bakhsh TA, Sadr A, Shimada Y, et al., 2013. Concurrent evaluation of composite internal adaptation and bond strength in a class-I cavity. *J Dent*, 41(1):60-70. https://doi.org/10.1016/j.jdent.2012.10.003

Bredbenner TL, Haug RH, 2000. Substitutes for human cadaveric bone in maxillofacial rigid fixation research. *Oral Surg Oral Med Oral Pathol Oral Radiol Endod*, 90(5):574-580. https://doi.org/10.1067/moe.2000.111025

Carrasco-Zevallos OM, Keller B, Viehland C, et al., 2016. Live volumetric (4D) visualization and guidance of *in vivo* human ophthalmic surgery with intraoperative optical coherence tomography. *Sci Rep*, 6:31689. https://doi.org/10.1038/srep31689

Choi KS, Wijesinghe RE, Lee C, et al., 2017. *In vivo* observation of metamorphosis of *Plodia interpunctella* Hübner using three-dimensional optical coherence tomography. *Entomol Res*, 47(4):256-262. https://doi.org/10.1111/1748-5967.12220

Fercher AF, Mengedoht K, Werner W, 1988. Eye-length measurement by interferometry with partially coherent light. *Opt Lett*, 13(3):186-188. https://doi.org/10.1364/OL.13.000186

Fernandes DJ, Elias CN, de Oliveira Ruellas AC, 2015. Influence of screw length and bone thickness on the stability of temporary implants. *Materials*, 8(9):6558-6569. https://doi.org/10.3390/ma8095322

Hsu JT, Chen YJ, Ho JT, et al., 2014. A comparison of micro-CT and dental CT in assessing cortical bone morphology and trabecular bone microarchitecture. *PLoS ONE*, 9(9):e107545. https://doi.org/10.1371/journal.pone.0107545

Huang D, Swanson EA, Lin CP, et al., 1991. Optical coherence tomography. *Science*, 254(5035):1178-1181. https://doi.org/10.1126/science.1957169

Katsumata A, Hirukawa A, Okumura S, et al., 2007. Effects of image artifacts on gray-value density in limited-volume cone-beam computerized tomography. *Oral Surg Oral Med Oral Pathol Oral Radiol Endod*, 104(6):829-836. https://doi.org/10.1016/j.tripleo.2006.12.005

Koprowski R, Machoy M, Woźniak K, et al., 2014. Automatic method of analysis of OCT images in the assessment of the tooth enamel surface after orthodontic treatment with fixed braces. *Biomed Eng Online*, 13:48. https://doi.org/10.1186/1475-925X-13-48

Lee NK, Baek SH, 2010. Effects of the diameter and shape of orthodontic mini-implants on microdamage to the cortical bone. *Am J Orthod Dentofacial Orthop*, 138(1):8.e1-8.e8. https://doi.org/10.1016/j.ajodo.2010.02.019

Melsen B, Costa A, 2000. Immediate loading of implants used for orthodontic anchorage. *Clin Orthod Res*, 3(1):23-28. https://doi.org/10.1034/j.1600-0544.2000.030105.x

Motoyoshi M, Inaba M, Ono A, et al., 2009. The effect of cortical bone thickness on the stability of orthodontic mini-implants and on the stress distribution in surrounding bone. *Int J Oral Maxillofac Surg*, 38(1):13-18. https://doi.org/10.1016/j.ijom.2008.09.006

Nackaerts O, Maes F, Yan H, et al., 2011. Analysis of intensity variability in multislice and cone beam computed tomography. *Clin Oral Implants Res*, 22(8):873-879. https://doi.org/10.1111/j.1600-0501.2010.02076.x

Nguyen MV, Codrington J, Fletcher L, et al., 2017. Influence of cortical bone thickness on miniscrew microcrack formation. *Am J Orthod Dentofacial Orthop*, 152(3):301-311. https://doi.org/10.1016/j.ajodo.2016.12.028

Park HS, Jeong SH, Kwon OW, 2006. Factors affecting the clinical success of screw implants used as orthodontic anchorage. *Am J Orthod Dentofacial Orthop*, 130(1):18-25. https://doi.org/10.1016/j.ajodo.2004.11.032

Park JY, Chung JH, Lee JS, et al., 2017. Comparisons of the diagnostic accuracies of optical coherence tomography, micro-computed tomography, and histology in periodontal disease: an *ex vivo* study. *J Periodontal Implant Sci*, 47(1):30-40. https://doi.org/10.5051/jpis.2017.47.1.30

Pithon MM, de Jesus Santos M, de Souza CA, et al., 2015. Effectiveness of fluoride sealant in the prevention of carious lesions around orthodontic brackets: an OCT evaluation. *Dental Press J Orthod*, 20(6):37-42. https://doi.org/10.1590/2177-6709.20.6.037-042.oar

Ravichandran NK, Wijesinghe RE, Shirazi MF, et al., 2016a. Depth enhancement in spectral domain optical coherence tomography using bidirectional imaging modality with a single spectrometer. *J Biomed Opt*, 21(7):076005. https://doi.org/10.1117/1.JBO.21.7.076005

Ravichandran NK, Wijesinghe RE, Shirazi MF, et al., 2016b. *In vivo* monitoring on growth and spread of gray leaf spot disease in capsicum annuum leaf using spectral domain optical coherence tomography. *J Spectrosc*, 2016:1093734. https://doi.org/10.1155/2016/1093734

Ravichandran NK, Wijesinghe RE, Lee SY, et al., 2017. Non-destructive analysis of the internal anatomical structures of mosquito specimens using optical coherence tomography. *Sensors (Basel)*, 17(8):1897. https://doi.org/10.3390/s17081897

Seeliger J, Machoy M, Koprowski R, et al., 2017. Enamel thickness before and after orthodontic treatment analysed in optical coherence tomography. *Biomed Res Int*, 2017: 8390575. https://doi.org/10.1155/2017/8390575

Shank SB, Beck FM, D'Atri AM, et al., 2012. Bone damage associated with orthodontic placement of miniscrew implants in an animal model. *Am J Orthod Dentofacial Orthop*, 141(4):412-418. https://doi.org/10.1016/j.ajodo.2011.10.021

Shirazi MF, Park K, Wijesinghe RE, et al., 2016. Fast industrial inspection of optical thin film using optical coherence tomography. *Sensors (Basel)*, 16(10):1598. https://doi.org/10.3390/s16101598

Shirazi MF, Wijesinghe RE, Ravichandran NK, et al., 2017. Dual-path handheld system for cornea and retina imaging using optical coherence tomography. *Opt Rev*, 24(2): 219-225. https://doi.org/10.1007/s10043-016-0288-5

Wawrzinek C, Sommer T, Fischer-Brandies H, 2008. Micro-damage in cortical bone due to the overtightening of orthodontic microscrews. *J Orofac Orthop*, 69(2):121-134. https://doi.org/10.1007/s00056-008-0742-5

Wijesinghe RE, Cho NH, Park K, et al., 2016. Bio-photonic detection and quantitative evaluation method for the progression of dental caries using optical frequency-domain imaging method. *Sensors (Basel)*, 16(12):2076. https://doi.org/10.3390/s16122076

Wijesinghe RE, Lee SY, Kim P, et al., 2017. Optical sensing method to analyze germination rate of *Capsicum annum* seeds treated with growth-promoting chemical compounds using optical coherence tomography. *J Biomed Opt*, 22(9): 091502. https://doi.org/10.1117/1.JBO.22.9.091502

Wilmes B, Rademacher C, Olthoff G, et al., 2006. Parameters affecting primary stability of orthodontic mini-implants. *J Orofac Orthop*, 67(3):162-174. https://doi.org/10.1007/s00056-006-0611-z

Woodall N, Tadepalli SC, Qian F, et al., 2011. Effect of miniscrew angulation on anchorage resistance. *Am J Orthod Dentofacial Orthop*, 139(2):e147-e152. https://doi.org/10.1016/j.ajodo.2010.08.017

Yadav S, Upadhyay M, Liu S, et al., 2012. Microdamage of the cortical bone during mini-implant insertion with self-drilling and self-tapping techniques: a randomized controlled trial. *Am J Orthod Dentofacial Orthop*, 141(5):538-546. https://doi.org/10.1016/j.ajodo.2011.12.016

Zhang Q, Lee CS, Chao J, et al., 2016. Wide-field optical coherence tomography based microangiography for retinal imaging. *Sci Rep*, 6:22017. https://doi.org/10.1038/srep22017

中文概要

题　目：使用光学相干成像技术对皮质骨植入微种植体产生微创的评估

目　的：评估光学相干成像技术（OCT）用于检测植入微种植体产生微创的效果，并将其与显微计算机断层扫描技术（μCT）进行对比，进一步验证 OCT 的检测效果。

创新点：采用两种成像技术进行比对，共同验证 OCT 的准确性和可行性。

方　法：将微种植体植入牛骨样品中，使用 OCT 和 μCT 成像。通过对比两种技术的成像来分析解剖学细节和微创面，从而判断 OCT 是否能够准确反映微种植体植入带来的微创。

结　论：OCT 能够生成高分辨率图片，清晰地反映微种植体周围产生的微创裂纹。与 μCT 生成的图像相比，由于 OCT 系统的高对比度和高分辨率，OCT 所生产的皮质骨表面图像质量高于正常标准。提高成像深度和开发口腔内部传感器对于发展实时成像系统并将其用于畸齿校正具有重大意义。

关键词：光学相干断层成像技术；微种植体；皮质骨；显微计算机断层扫描技术